

Evidence for different polymorphisms with and without an external electric field in a series of bent-shaped molecules

J. P. Bedel, J. C. Rouillon, J. P. Marcerou, H. T. Nguyen, and M. F. Achard*

Centre de Recherche Paul Pascal, CNRS, Université Bordeaux I, 115 Avenue A. Schweitzer, 33600 Pessac, France

(Received 29 July 2003; revised manuscript received 13 November 2003; published 1 June 2004)

Five fluid tilted mesophases are observed in a series of achiral banana-shaped compounds. The terminal chain length is the pertinent molecular parameter which induces the polymorphism change. All the phases, refer to tilted lamellar structure without in-plane order in the layers. The observation of monolayer, bilayer, ribbon phase, and undulated structures recalls the richness of the polymorphism of the frustrated polar calamitic liquid crystals. Among the mesophases, we highlight two: a $Sm-CG_2$ phase corresponding to a bilayer structure made of $Sm-CG$ layers, and its two-dimensional variant, $Sm-\tilde{C}G_2$. The five mesophases observed at zero field are switchable under electric field. At least three ferroelectric phases are induced by an applied field. There is no direct correspondence between the zero field phases and the phases observed under electric field. These observations show that different polymorphisms exist in the series with and without an applied field. A unique (E, T) phase diagram is presented, corresponding to the superposition of the (E, T) diagrams obtained for each homolog of the series, where the influence of the chain length is equivalent to a shift on the temperature axis.

DOI: 10.1103/PhysRevE.69.061702

PACS number(s): 61.30.Eb, 64.70.Md, 77.84.Nh

I. INTRODUCTION

For several decades, the molecular shape of liquid crystalline materials has been restricted to rodlike or disklike units, and with these basic forms it was rather easy to imagine nematic, smectic, or columnar arrangements. Nevertheless, the inventive action of chemists led to the synthesis of new materials with more complicated anisotropic form and as a result, the complexity of the mesomorphic arrangements increased. An illustrative example of this situation concerns bent-shaped (or “banana-shaped”) molecules. This molecular geometry may provoke a polar packing within the layers, at least at short range, which can generate ferroelectric properties [1,2]. Depending on the arrangement of the bent molecules in smectic layers, different classes of fluid mesophases were predicted [3–5] according to different symmetries. A smectic phase with triclinic symmetry, the lowest possible symmetry ($C1$), was prognosticated by de Gennes [6], and banana-shaped molecules are good candidates to give experimental evidence for this prediction [7–10]. Thus these materials can adopt complex arrangements and form new mesophases [11]. It was first proposed at the Workshop on Banana-shaped Liquid Crystals (Berlin, 1997) to use the label Bn for these mesophases (with the index n corresponding to the sequence of their discovery). Nevertheless, with increasing the number of materials, this nomenclature appears insufficient and recently scientists in the liquid crystal field initiated the process of formalizing the nomenclature of banana liquid crystals (Banana Liquid Crystals—Chirality & Polarity, Boulder, 2002) [12].

In this paper, we report results which peculiarly illustrate the complexity of the mesomorphic behavior of banana-

shaped liquid crystals: in the same series, five mesophases are distinguished according to the terminal chain length. All are switchable under electric field, leading to at least three different ferroelectric phases. At the moment, it is difficult to generalize the influence of the terminal chain length on the formation of different mesophases in banana materials. Nevertheless, with numerous series synthesized in our group and not published yet, as well as with the data reported in the literature [11,13–17], the effect of this molecular parameter on the liquid crystalline behavior of banana-shaped compounds is unusually strong (and not universal) in comparison with calamitic liquid crystals.

In the following, we present the evolution of the mesomorphic, structural and electric behaviors versus the terminal chains length n in this homologous series (E_n).

II. MATERIALS

Experiments were carried out on a series of banana-shaped molecules, the bis[4-(4- n -alkyloxycarbonylbenzylideneamino)]phenyl isophthalate series previously synthesized [17]. The materials are labeled “ E_n ”, where n is the number of carbon atoms in the terminal ester chain ($n = 7–16$) and correspond to the chemical formula of Fig. 1.

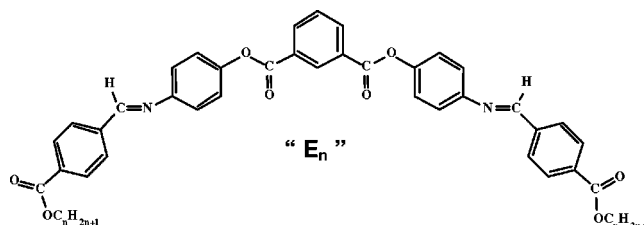


FIG. 1. Chemical structure of the E_n compounds.

*Corresponding author. Email address: achard@crpp-bordeaux.cnrs.fr

TABLE I. Transition temperatures ($^{\circ}\text{C}$) vs the terminal chains length n in the E_n series. Transition enthalpies (J g^{-1}) are in italics. For phase identification see text. [] indicates a monotropic transition.

n	K	Sm- $C_S P_A$	Sm- $C_S G_2 P_A$	Sm- $\tilde{C}_S G_2 P_A$	Sm- CP_A	Sm- $CU P_A$	I
7	• 183.9	• 190.6					•
	43.8	19.7	-	-	-	-	
8	• 178.6	• 187.8					•
	37.0	18.9	-	-	-	-	
9	• 174.0	• 184					•
	36.8	20.3	-	-	-	-	
10	• 173.5	• 180	• 183.5				•
	40.8	0.2	20.4	-	-	-	
11	• 172.0			• 181.9			•
	38.5	-	-	21.3	-	-	
12	• 174.4			• 182.7			•
	39.8	-	-	21.1	-	-	
13	• 170.5			• 178.5			•
	42.4	-	-	21.3	-	-	
14	• 169.6			• 176.9			•
	44.5	-	-	21.1	-	-	
15	• 167.9				• 171.4	• 174.3	•
	45.3	-	-		0.54	20.7	
16	• 166.9				• [153.7]	• 172.6	•
	43.7	-	-		0.44	19.5	

III. EXPERIMENTAL

The thermal behavior was investigated using a Perkin-Elmer DSC7 differential calorimeter.

The optical textures were observed through a polarizing microscope (Leitz Diavert) equipped with a hot stage (FP-82HT) and an automatic controller (Mettler FP-90). Samples are observed on regular slide glass without any surface treatment.

X-ray diffraction experiments were carried out on a 18 kW rotating anode x-ray source (Rigaku-200) with use of Ge (111) crystal as monochromator. The scattered radiation was collected on a two-dimensional detector (Imaging Plate system from Mar Research, Hamburg). The samples were placed in an oven, providing a temperature control of 0.1 K. Oriented samples were obtained by slowly cooling down a drop of the isotropic liquid.

Electro-optical properties were studied using commercial cells (from E.H.C., Japan). Switching current was observed by applying a periodic voltage wave using a function synthesizer (HP 33120A) and a high power amplifier (Krohn-Hite). Square-wave, triangular, or more complicated ac voltages shapes were used at low frequency (1–100 Hz). To follow the textural changes during the polarization switching process a stroboscopic setup was used: a video camera (Sony XC-003P) took 1 ms exposure time images at a frequency of 50 Hz while the ac voltage was set close to this frequency.

IV. STRUCTURES

The characterization of the phases based on x-ray diffraction measurements and optical observations reveals the exist-

ence of five mesophases in the series depending on the carbon number in both terminal chains (Table I): the homologs with the shortest chains (E_7 – E_9) exhibit one lamellar phase, two smectic phases are observed for the E_{10} compound, a two-dimensional phase exists for the intermediate chains ($n = 11$ to 14), while the longer homologs exhibit two mesophases, one two-dimensional phase and one smectic phase. Note that such a rich polymorphism is rather unusual in the banana-shaped series already reported in the literature. In the following, we adopt a simple nomenclature Sm- CP (instead of “Bn”), where Sm- C means a fluid tilted lamellar phase and P signifies that the phase is switchable under electric field. Additional subscripts will modify and complete this basic appellation, for example, C_S/C_A for synclinic/anticlinic tilt, P_A/P_F for antiferroelectric/ferroelectric polarization distribution [2].

A. Short homologs $n=7-10$

Short homologs ($n=7-10$) display the same mesophase [17]. Oriented x-ray patterns give evidence of a tilted smectic phase with no long range positional order within the layers. The tilt angle is around 25° , the layer spacing $d=2\pi/q_1$, where q_1 is the wave vector, is close to the molecular length and linearly increases with the carbon number in the terminal chain n (42.2 Å for $n=7$, 43.9 Å for $n=8$, 44.9 Å for $n=9$, and 46.5 Å for $n=10$). The small increment of d per methylene group shows that the chains are tilted with respect to the layers. This mesophase is switchable under electric field after a significant threshold. In this sense, it has probably no

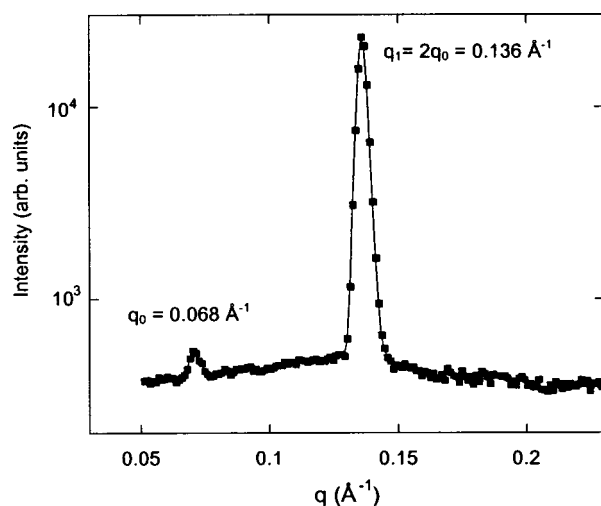


FIG. 2. Intensity profile in the small angle region of the bilayer Sm-CG_2 phase of the E_{10} compound. The intensity of the peak corresponding to the bilayer reflection is about 100 times weaker than for the monolayer reflection.

macroscopic polarization and thus enters the Sm-CP_A class.

The most exciting result concerns the E_{10} homolog [17] which displays another tilted smectic phase with a two-layer structure instead of a monolayer one as observed for the other short homologs. The oriented x-ray pattern exhibits a peak of low intensity located on the meridian at $q_0 = 0.068 \text{ \AA}^{-1} = 2\pi/92 \text{ \AA}^{-1}$ while an intense peak corresponding to the “monolayer” reflection remains at $q_1 = 2q_0 = 0.136 \text{ \AA}^{-1} = 2\pi/46 \text{ \AA}^{-1}$ (Fig. 2). The phase transition to the lower-temperature mesophase corresponds to a bilayer-monolayer phase change.

Conventional x-ray diffraction is normally unable to detect a two-layer superlattice when the projection of the electron density along the layer normal z is identical for successive layers. It was the case of chiral Sm-C^* variants of rodlike mesogens for which two-layer, three-layer, and four-layer structures have been only evidenced by resonant x-ray diffraction [18,19] and it is probably also the case for phases belonging to the Sm-CP_A class. Indeed the same technique recently revealed a two-layer periodicity for a material exhibiting a B2 phase [20]. Thus the detection of a two-layer structure by conventional x-ray diffraction supposes a dissymmetry of two successive layers. This opportunity could originate from the shape of the banana molecule itself which generates many possible stackings in the layers. A classical representation of a banana molecule is a bow with the director \mathbf{l} pointing from end to end, the polar axis \mathbf{p} corresponding to the bow’s arrow, and the \mathbf{m} axis perpendicular to the molecular plane. In most tilted fluid smectic phases observed in banana mesogens, at least one of the axes lies within the smectic layers. Nevertheless, the possibility of smectic phases with triclinic symmetry, i.e., the lowest symmetry, was predicted by de Gennes [6] and was named smectic CG phase, where G stands for generalized. An orientation of the bananas where all three principal axes make an angle with the smectic layers different from 0° or 90° (Fig. 3) leads to the smectic CG phase. Experimental evidence for this triclinic symmetry of a smectic phase of banana-shaped mol-

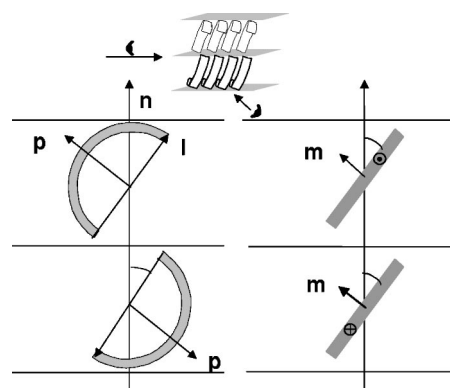


FIG. 3. Sketch of the synclinic stacking in the bilayer $\text{Sm-C}_5\text{G}_2\text{P}_A$ phase. On the left, the molecular long axis is inclined by the leaning angle, and on the right, the molecular plane is tilted by the tilt angle.

ecules has been recently reported [7–10]. The association of two Sm-CG layers with alternating leaning angles can generate a z -projected electron density corresponding to a two-layer modulation which should be detected with conventional x ray. Brand *et al.* [4] described eight different possibilities that emerge when two layers of different forms of Sm-CG are associated and four of them correspond to a bilayer modulation. According to these arguments, the high-temperature phase of the $n=10$ compound is thus a good candidate to be a Sm-CG_2 , where the subscript 2 stands for a bilayer structure made of Sm-CG layers. As previously reported [17], the Sm-CG_2 observed in the E_{10} compound is switchable under electric field. Within the smectic CG_2 ’s two-layer stackings [4], we choose a structure corresponding to a macroscopic polarization equal to zero since its creation only occurs after a significant threshold ($5 \text{ V}/\mu\text{m}$). This stacking is antiferroelectric and corresponds to a synclinic arrangement with the same tilt angle from one layer to the other (Fig. 2) with an alternating leaning angle. The high-temperature phase of the E_{10} compound can thus be labelled $\text{Sm-C}_5\text{G}_2\text{P}_A$.

The isotropic- $\text{Sm-C}_5\text{G}_2\text{P}_A$ transition is strongly first order while the $\text{Sm-C}_5\text{G}_2\text{P}_A$ – Sm-CP transition induced by decreasing the temperature corresponds to a very weak enthalpy change. This last transition corresponds to the disappearance of the q_0 reflection and by a slight increase of the “monolayer” spacing which is consistent with a rotation of the molecules around \mathbf{m} the leaning angle, which corresponds to the inclination of the long axis in the tilt plane, vanishes. Thus, the $\text{Sm-C}_5\text{P}_A$ label can be adopted for E_7 – E_9 mesophase and the low-temperature phase of E_{10} .

B. Intermediate homolog $n=11$ – 14

For intermediate chain length ($n=11$ – 14) the diffuse spots at wide angles confirm the liquidlike order of the molecules inside the layers with a tilt angle around 20° . In the small angle region, the spot at q_0 (001) corresponding to the “bilayer” structure splits into two spots (101) located out of the meridian (z axis) while the “monolayer” (002) spot at q_1 remains with a strong intensity [Figs. 4(a) and 4(b)]. Along z

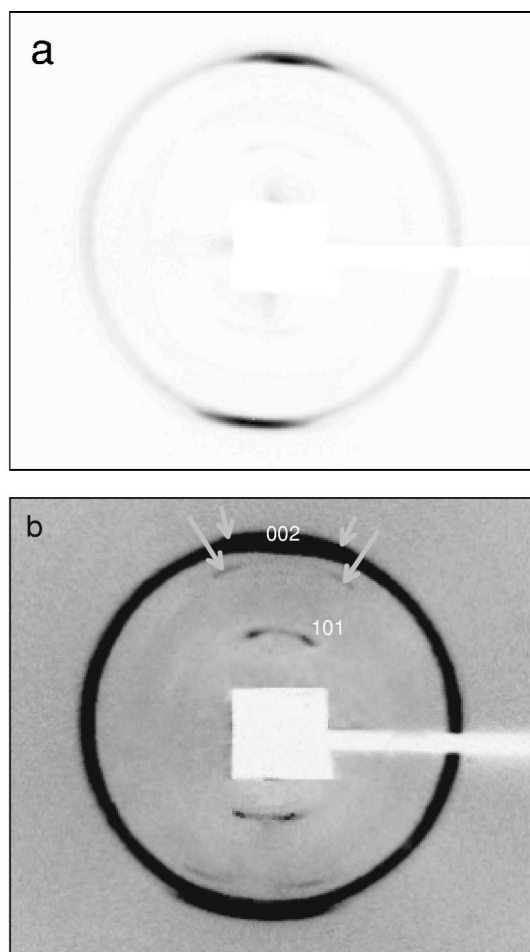


FIG. 4. Oriented x-ray pattern of the E_{14} compound in the small angle region. (a) With a short exposure time, very intense spots located on the meridian z are observed. (b) With longer exposure times these spots are overexposed and four additional spots located out of the meridian are clearly seen. The arrows indicate hardly visible extra spots.

the two wave vectors remain commensurate (the z component q_{0z} of q_0 is equal to $q_1/2$). The splitting of the first reflection into the 101 spots is a clear indication of a two-dimensional ribbonlike structure [21] and the bilayer structure built with two associated Sm- CG layers, is now periodically broken by oblique defect walls which are most probably facilitated by the synclinc arrangement of the tilted molecules.

The wavelength of the modulation along the layers ($2\pi/q_{0x}$) increases from $n=14$ to $n=11$ (300 Å for $n=14$, 700 Å for $n=12$, and $\gg 1000$ Å for $n=11$) (Fig. 5) and the lateral modulation collapses for $n=10$, i.e., the wavelength tends to infinity. The bilayer smectic Sm- $C_sG_2P_A$ phase of the E_{10} compound is thus the commensurate limit of the ribbon phase labeled Sm- $\tilde{C}_sG_2P_A$ observed for E_{11} – E_{14} . The observed spherulitic textures (Fig. 6) which are reminiscent of columnar or Sm- \tilde{C} ribbon phase are also consistent with this identification.

As for Sm- \tilde{C} or Sm- \tilde{A} phases [21,22], we cannot decide between one- or two-dimensional modulations within the

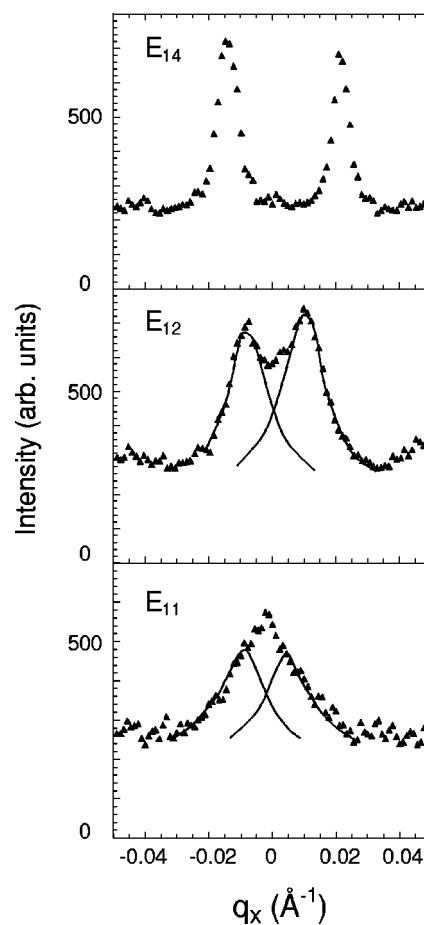


FIG. 5. X-ray intensity profiles as a function of q_{0x} at constant q_{0z} : the wavelength of the modulation along the layers ($2\pi/q_{0x}$) increases from $n=14$ to $n=11$.

layers. Indeed, due to the method used to align these banana compounds, the x-ray pattern has a cylindrical symmetry around the axis of the droplet (z axis) and leads to a monodomain along the z axis, i.e., the layers are parallel to the substrate and to polydomains in the (x,y) plane perpendicular to this axis, i.e., the tilt and/or leaning angles are not uniform. In addition, in the absence of a real monodomain, the faint visible additional spots [Fig. 4(b)] which project on

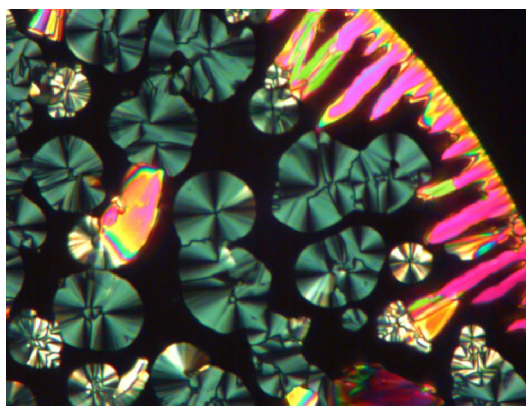


FIG. 6. (Color online) Example of the spherulitic texture observed for E_{14} at 174°C.

the q_0 direction at $q_0\sqrt{3}$ and at $q_0\sqrt{4}$ cannot be undoubtedly indexed.

What is the origin of the frustration in banana compounds which induces such 2D mesophases? As extensively developed for smectic phases of polar rodlike mesogens [23–25], the coexistence of two periodically modulated order parameters with different preferred wave vectors can lead to a set of phases when these two wave vectors adopt commensurate or incommensurate values.

The first order parameter is the smectic one, i.e., the periodic modulation of matter density defining the layers: $\delta\rho e^{iq_1z}$ (z is the layer normal). The second one is the polarization density wave (PDW) which is the average of the local polarization, computed at the same scale as $\delta\rho$. In general, the PDW is a vector with three periodic components $p_x e^{i(q_x r + \varphi_x)}$, $p_y e^{i(q_y r + \varphi_y)}$, $p_z e^{i(q_z r + \varphi_z)}$ [26]. In these expressions, the p_i moduli have the dimension of a charge per unit surface and some of them should be large in case of a switchable phase. The direction of modulation r should be the layer normal z for flat smectic phases. In that case, the wave vectors q_i should be integer submultiples of the layer fundamental q_1 . Finally, the value of the phase φ_i determines if the PDW component is in phase or in quadrature with the density wave $\delta\rho$, respectively, maximum in the middle of a layer or in the interlayer plane. In banana lamellar mesophases, as in the case of polar smectics [27], the PDW has to adopt a periodicity and phase compatible with the smectic order parameter. In bilayer phases, a coupling term of the form $p^2 \delta\rho^*$ in the free energy density [25] governs the interaction and imposes a locking of the wave vector of the PDW to half the value of q_1 . For example, in a bilayer Sm- C_5P_A phase (synclinic tilt of the director in adjacent layers and antiferroelectric relation between successive layers, y being the direction of the in-plane polarization), one gets $r=z$, $q_x=q_z=q_1$, $\varphi_x=\varphi_z=\pi/2$, $q_y=q_1/2$, $\varphi_y=0$ or π . In a bilayer Sm- $C_5G_2P_A$ phase, one gets $r=z$ the layer normal, $q_x=q_1$, $\varphi_x=\pi/2$, $q_y=q_z=q_1/2$, $\varphi_y, \varphi_z=0$ or π . If the commensurability between q_1 and the wave vectors q_y and q_z cannot be ensured anymore, there is a possibility of escaping the problem by making an antiphase Sm- $\tilde{C}_5G_2P_A$ with p_y and p_z modulated along r at an angle with z such that the projection along z of q_y and q_z be $q_1/2$ with again $\varphi_y, \varphi_z=0$ or π . Thus the mesophases of banana compounds can be described with a generalization of the basic equations used for frustrated phases of polar rods [23–25].

C. Long homologs $n=15, 16$

For longer chains, two mesophases are observed. The high-temperature phase forms smooth domains and the low-temperature phase is readily distinguished by its striated texture.

The x-ray diffraction pattern of aligned sample shows diffuse spots at wide angles, located out of the equator corresponding to a tilt angle of $\sim 10^\circ$. In the small-angle region, the patterns of the high-temperature phase [Fig. 7(a)] show a lamellar structure with a layer spacing close to the molecular length ($q_1=0.116 \text{ \AA}^{-1}=2\pi/54.1 \text{ \AA}$ for $n=15$ and $q_1=0.113 \text{ \AA}^{-1}=2\pi/55.6 \text{ \AA}$ for $n=16$). Satellites are visible

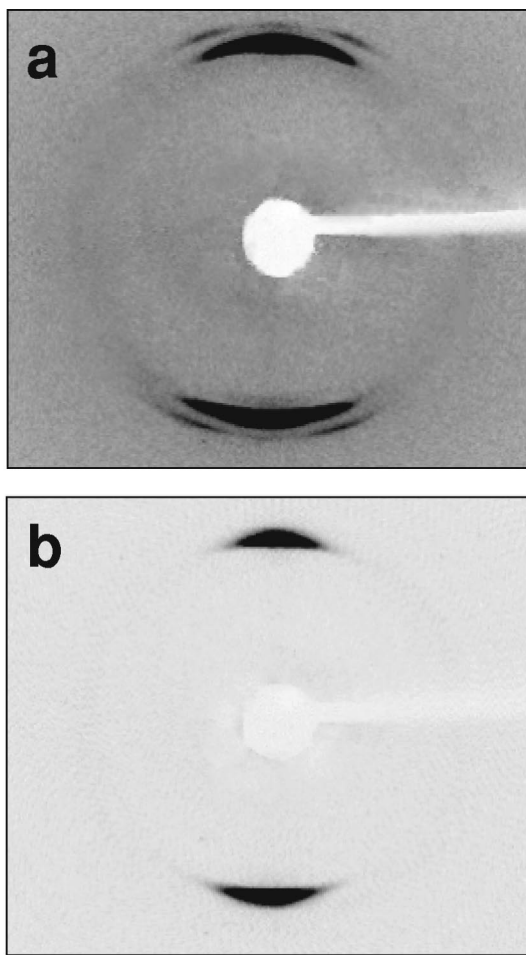


FIG. 7. Oriented x-ray patterns of the E_{15} compound. (a) Undulated Sm- CUP_A phase (173°C). (b) In the low-temperature phase (167°C), the satellites disappear giving rise to a Sm- CP_A phase.

around q_1 out of the meridian. They correspond to a 2D modulation in the layer plane with a periodicity of around 150 \AA . This structure corresponds to a “monolayer” undulation and we label the phase Sm- $CU P_A$ (where U stands for undulated). At lower temperature, the satellites disappear [Fig. 7(b)] giving rise to a tilted smectic phase labeled Sm- $C P_A$.

V. ELECTRO-OPTIC STUDIES

Five mesophases have been observed in this series depending essentially on the chain length and at lesser extent on temperature. Their structures have been determined by x-ray diffraction and they correspond to the thermodynamically stable mesophases in absence of any applied electric field ($E=0$).

These five mesophases are switchable under electric field after a threshold ranging from $1\text{--}7 \text{ V}/\mu\text{m}$. These rather large thresholds imply that the macroscopic polarization of the initial phases (at $E=0$) is identically null and a simple way to ensure this condition in a layered phase where a pre-order of the dipoles exists is to assume that this pre-order is of

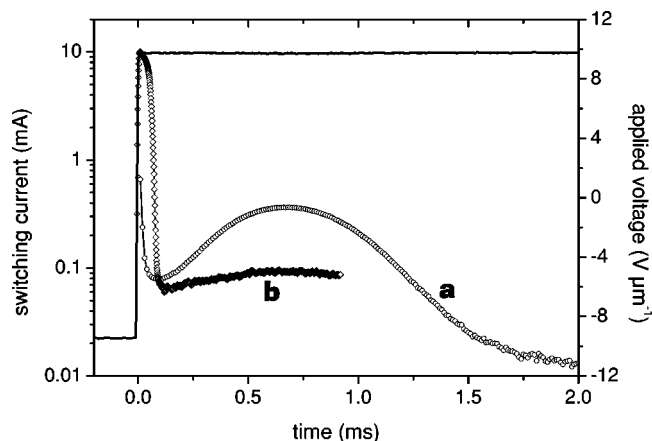


FIG. 8. Typical responses to a square wave voltage above the threshold(s) (a) of a “classical ferroelectric” where the uniform macroscopic polarization rotates in space with a short delay after the voltage switching and (b) of a “nonclassical ferroelectric” with a nonuniform polarization that begins to rotate immediately after the switch. Note the large difference in the two time scales. In both cases, the polarization is large (a few hundred nC cm^{-2}).

the “antiferroelectric” type. This justifies the adjunction of the *A* suffix in the phase denomination in accordance with the Workshop nomenclature in preparation at the time of writing [12].

So within the set of PDWs, we assume that there exists one in-plane wave $p_y e^{iq_1(z/2)}$ for the “antiferroelectric” Sm-CP_A phases and, together with it, an additional one $p_z e^{iq_1(z/2)}$ normal to the layers for the $\text{Sm-C}_5G_2P_A$ with a period corresponding to the bilayer structure. For the $\text{Sm-C}_5G_2P_A$ phase, these PDWs are both modulated along a direction *r* making an angle with *z*.

These PDWs may be considered as precursors of the macroscopic polarization of the new phases obtained under field after a phase transition occurring at the threshold field E_{th} . As shown below, three different ferroelectric phases were induced under the applied field in this series.

Depending on the chain length (*n*), the temperature (*T*), and the electric field strength (*E*), different basic electro-optic responses were characterized. The thresholds E_{th} above which the ferroelectric phases appear, were determined under square-wave fields (Fig. 8), and plotted in a (*E*, *T*) phase diagram [28] for each compound as they represent a first approximation of the phase boundaries in such a diagram. The appearance/disappearance of the ferroelectric phases by increasing/decreasing the field is reversible.

Two kinds of responses to a square-wave excitation were observed: the first one is characteristic of a “classical” ferroelectric behavior where the polarization rotates uniformly in space after a delay [Fig 8(a)]; the second corresponds to a “nonclassical” ferroelectric where the polarization begins to rotate immediately after the voltage switching leading to the current shape of Fig. 8(b). A material composed of ferroelectric grains whose polarizations are not perfectly parallel, and where some of them rotate just after the field sign change, could give such kind of response.

The stability of the induced phases was characterized by the shape of the polarization current slowly varying the field

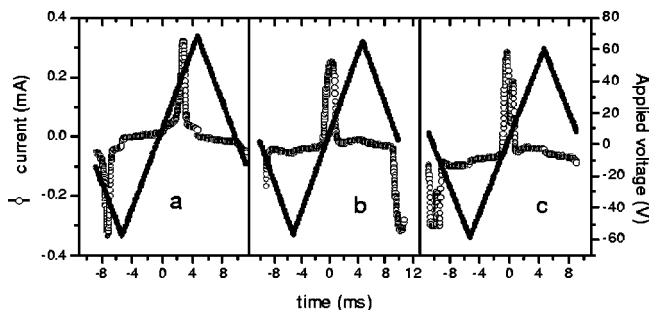


FIG. 9. Typical responses to a triangular wave voltage above the threshold(s) (a) of a “classical ferroelectric” with a short delay after the voltage zero crossing, (b) of a “nonclassical ferroelectric” with a nonuniform polarization that rotates symmetrically around the zero crossing (“superparaelectric” behavior [29]), and (c) of a “nonclassical ferroelectric” with a nonuniform polarization that reorients in two steps.

together with the observation of the textures with a stroboscopy setup. Under a triangular-wave excitation, the uniformly polarized phases lead to a classical delayed peak [Fig. 9(a)] while two “nonclassical” ferroelectric responses were observed: the “superparaelectric” behavior of Fig. 9(b) where the polarization sign changes continuously in the vicinity of the zero crossing [29] and a hybrid case, where the polarization vanishes just before the zero crossing and reappears after a slight threshold [Fig. 9(c)]. One must point out that the classical “antiferroelectric” behavior corresponding to two well separated peaks in triangular voltage and one delayed peak in square wave [Fig. 8(a)] was never observed in this series.

To sum up, the response “8b” under square-wave voltages together with the cases “9b” or “9c” under triangular voltage corresponds to nonuniformly polarized phases that we get together with the “nonclassical ferroelectric” label.

The response “8a” with a square-wave excitation together with the response “9a” under triangular voltage corresponds to a uniformly polarized phase, namely, a “classical ferroelectric.” Nevertheless, with this same electric behavior, two different “classical ferroelectric” phases were clearly distinguished in this series according to their optical responses.

(i) One, with an optical texture showing a splitting in switching domains of opposite chirality (Fig. 10), that we identify to the $\text{Sm-C}_5P_F^*$ of the NOBOW compound [2,30]. It corresponds to the characteristic switching of a chiral Sm-C^* where both the long axis of the molecules and the polarization rotate around the layer normal [Fig. 11(a)]. Domains of opposite chirality coexist under the form of stripes or maltese crosses. These domains are bistable as the optical axis remains unchanged on removing the field for a short time. When the field is definitively removed the stripes disappear. Polarizations *P* up to 430 nC/cm^2 are observed.

(ii) The other showing a degenerate planar texture independent of the polarity of the field, i.e., with the same direction of the optical axis for both field signs. Due to the continuity of the birefringence colors (reddish with $3.5 \mu\text{m}$ thickness cell) when one goes from this phase to the $\text{Sm-C}_5P_F^*$ phase at higher field, we cannot assert it to be of the $\text{Sm-C}_A P_A$ kind like in NOBOW compound as it would be an

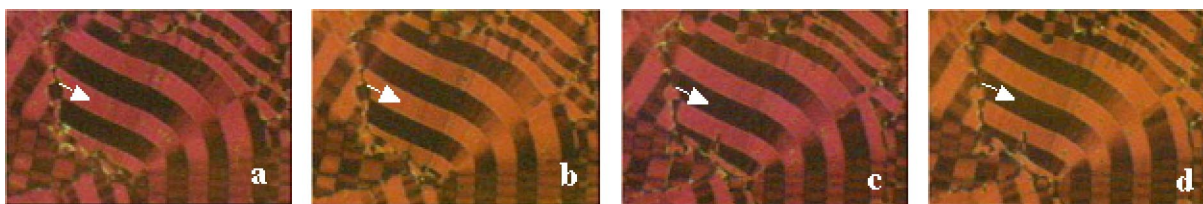


FIG. 10. (Color online) Textures of the $Sm-C_5P_{F^*}$ phase encountered after a second threshold in E_{16} at $168^\circ C$. The voltage shape was of the “staircase” kind with a constant voltage during one-fourth of the period (20 ms) at values $+V$, 0 , $-V$, and 0 . (a) At $+V$ the sample is equally divided in black (optical axis parallel to the polarizer) and pink (axis at an angle) stripes evidencing the domains of opposite chirality. (b) At $0V$ on the next plateau, the optical axes stay in the same direction while the birefringence color changes to orange (c) At $-V$ the directions of optical axes are swapped between domains of opposite chirality, the color reverts to pink. (d) At $0V$ the axes stay in the new direction (bistability of the $Sm-C_5P_{F^*}$ phase) while birefringence color is orange again. When the field is definitively removed the stripes disappear but the birefringence color is kept.

antclinic phase with a smaller birefringence and a greenish color. We assume it to be also a synclinic tilted phase, without the splitting in domains of opposite chirality, we label this phase “achiral $Sm-C_5P_F$ ”. The optical properties imply that the polarization switches by rotating around the optical axis [Fig. 11(b)] as already reported in banana compounds [31,32] which is forbidden in chiral smectics of rodlike molecules. Moreover, if the switching mechanism sketched in Fig. 11(b) is correct, the layers cannot be considered as chiral, or maybe the field reversal could lead to a change in the chirality sign. Polarization is about 330 nC/cm^2 .

Which phases are encountered when one passes a field threshold? On average, in this series, one observes a unique threshold at a few $V/\mu m$ with the shortest chains, while the longest homologs show two successive thresholds at higher voltages. When there is only one threshold, the phase under field is always a “nonclassical ferroelectric” phase as defined before. When two thresholds are evidenced, the phase at lower field is always an achiral $Sm-C_5P_F$, while at higher field the phase may be either a “nonclassical ferroelectric” phase for short chains or a chiral uniform ferroelectric $Sm-C_5P_{F^*}$ for long homologs. Nevertheless, the separation between these different electro-optic responses is not abrupt

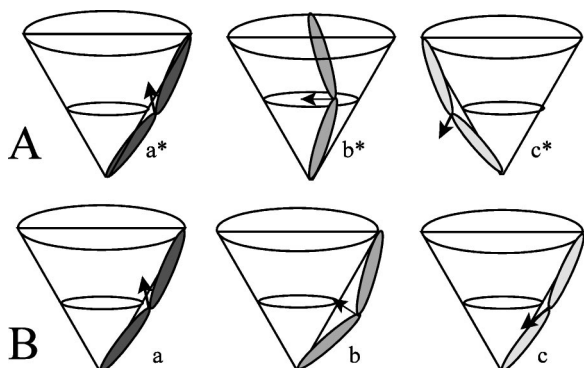


FIG. 11. Schematic mechanisms of the switching of the polarization under a field reversal in (a) the $Sm-C_5P_{F^*}$ (the polarization rotates around the layer normal) and (b) nonchiral $Sm-C_5P_F$ (the polarization rotates around the molecular axis). The cases labeled (a^* , a) correspond to a field pointing backward, (c^* , c) to forward, and (b^* , b) to an intermediate position during the polarization switching.

and does not coincide with an increment of the terminal chain length n . Thus, contrarily to the generally received opinion, it is obvious that there is no direct correspondence between the behavior under field and the nature of the mesophase at zero field. As an illustrative example, one can note that all these electro-optic behaviors can be successively observed versus temperature in a pure compound (E_{14}), although it presents only one phase at zero field: thus increasing the field, a $Sm-\tilde{C}_5G_2P_A \rightarrow Sm-C_5P_F \rightarrow Sm-C_5P_{F^*}$ sequence is observed at high temperature ($T_{im}-T=0-10^\circ C$, where T_{im} is the isotropic liquid–mesophase transition temperature), a $Sm-\tilde{C}_5G_2P_A \rightarrow Sm-C_5P_F \rightarrow$ “nonclassical ferroelectric phase” sequence exists for intermediate temperatures ($T_{im}-T=10-20^\circ C$), and at low temperature ($T_{im}-T=20-30^\circ C$) a direct $Sm-\tilde{C}_5CSG_2P_A \rightarrow$ “nonclassical ferroelectric phase” transition occurs. A field-temperature phase diagram summarizes these complex responses of the E_{14} compound under electric field (Fig. 12).

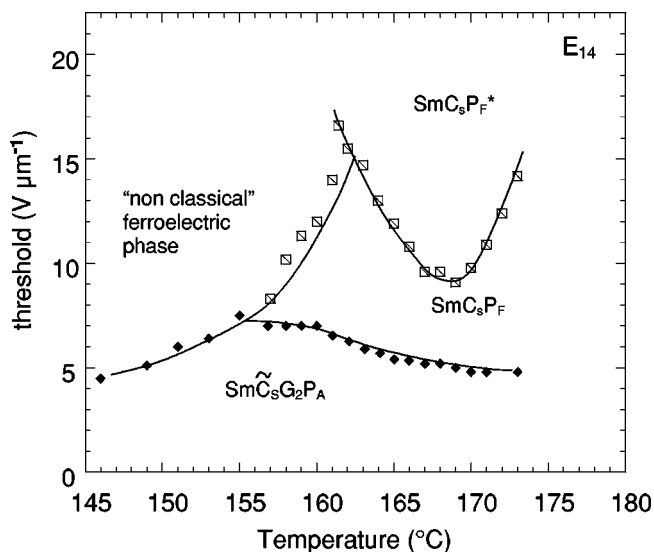


FIG. 12. (E, T) phase diagram for a pure compound (E_{14}) showing a single phase at zero field. The electric field thresholds corresponding to the phase transitions are plotted vs temperature. Depending on the temperature and on the electric field strength, three different ferroelectric phases are induced (see the text).

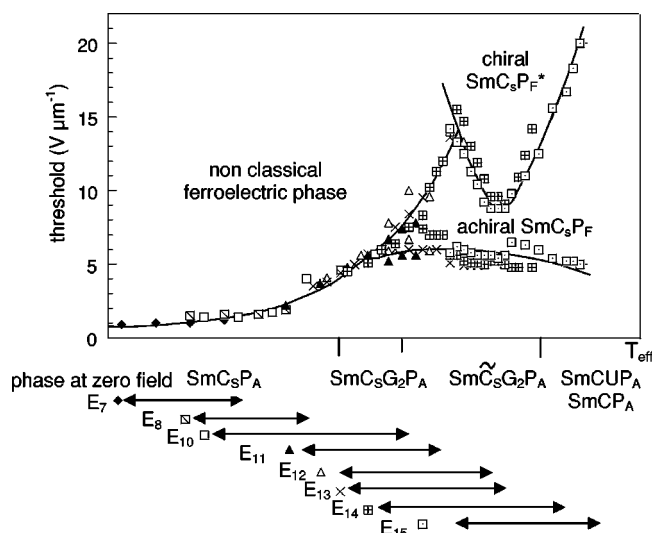


FIG. 13. General (E, T) phase diagram including all the compounds of the series. The electric field thresholds (in $V \mu\text{m}^{-1}$) corresponding to the phase transitions are plotted vs an effective temperature T_{eff} which is determined by shifting the experimental temperature by an amount depending on the chain length “ n ”. Different symbols were assigned to the compounds and the corresponding temperature range explored between the isotropic phase and the crystal is schematized by the arrows below the figure. The five zero field phases are mentioned on the $E=0$ line.

Correlatively in the series, there is also a continuous evolution of the electro-optic response versus the chain length. Thus, when one compares the different phase diagrams [nature of the induced ferroelectric phase(s) and threshold values], the behavior of compound n at a given temperature is similar to that of compound $n+1$ at a lower temperature. These observations allow us to draw a unique (E, T_{eff}) phase diagram representative of the whole series (Fig. 13): this diagram is obtained by superposition of the individual phase diagrams with a suitable shift on the temperature axis depending on the chain length (surprisingly, this temperature shift is linear with n). Thus the nature and number of the ferroelectric phases induced by the field and the values of the threshold(s) can be easily derived for each compound from this unique diagram. It may be only considered as a guide for summarizing the data but is reminiscent of known results in liquid crystals where changing the chain length is equivalent to a pressure or temperature shift for a given compound.

Nevertheless, it is obvious from this general diagram that there is no direct relation between a thermodynamically stable phase at zero field and the electro-optic response under field: a phase at zero field may transform in different mesophases under field, and at the opposite a mesophase observed under field can originate from different mesophases at zero field.

VI. CONCLUSION

To sum up, among the five fluid mesophases encountered in this series of achiral banana-shaped molecules, a two-layer structure (Sm-CG_2) made of Sm-CG layers was found. The so-called Sm-CG phase predicted by de Gennes is the most general tilted smectic phase that is fluid in the layers with triclinic symmetry and is characterized by two tilt directions with respect to the layer normal, tilt of the molecular plane (clinic) and tilt of the molecular kink directions (leaning). In a theoretical investigation, Brand *et al.* [4] described the left-handed and right-handed versions of the Sm-CG and showed different possibilities that emerge when two layers of different forms are associated and several candidates for a Sm-CG structure have been already reported in banana compounds [7–10]. Here the proof of a bilayer structure possible because of the leaning angle is an important result of this study. Interestingly, as for frustrated polar calamitic liquid crystals [25], this two-layer $\text{Sm-C}_5\text{G}_2\text{P}_A$ structure appears as the commensurate limit of a two-dimensional ribbon phase $\text{Sm-C}_5\tilde{\text{G}}_2\text{P}_A$. Here the frustration can be described with the basic equations used for polar rods by using two order parameters, namely, the periodic modulation of matter density defining the layers and the polarization density waves. With these basic ingredients it would be possible to theoretically generate the same richness of polymorphism in banana molecules as in polar rods.

The five thermodynamically stable mesophases are switchable under electric field. Three ferroelectric phases, including a chiral $\text{Sm-C}_5\text{P}_F^*$, are observed under field and the whole results of the En series can be summarized in a general field-temperature phase diagram. At last, it is obvious from these results that two different polymorphisms exist with and without electric field and that there is no direct correspondence between the phases at zero field and phases observed under field. X-ray experiments are currently in progress to investigate the structure of the mesophases induced under electric field.

[1] T. Niori, T. Sekine, J. Watanabe, T. Furukawa, and H. Takezoe, *J. Mater. Chem.* **6**, 1231 (1996).
 [2] D. R. Link, G. Natale, R. Shao, J. E. MacLennan, N. A. Clark, E. Körblova, and D. M. Walba, *Science* **278**, 1924 (1997).
 [3] H. R. Brand, P. E. Cladis, and H. Pleiner, *Macromolecules* **25**, 7223 (1992).
 [4] H. R. Brand, P. E. Cladis, and H. Pleiner, *Eur. Phys. J. B* **6**, 347 (1998).

[5] A. Roy, N. V. Madhusudana, P. Toledano, and A. M. Figueiredo Neto, *Phys. Rev. Lett.* **82**, 1466 (1999).
 [6] P. G. de Gennes, *The Physics of Liquid Crystals* (Clarendon Press, Oxford, 1974), p 277.
 [7] <http://www.lci.kent.edu/ALCOM/symposiaanniversary.html>
 [8] A. Jákli, D. Krüerke, H. Sawade, and G. Heppke, *Phys. Rev. Lett.* **86**, 5715 (2001).
 [9] A. Eremin, S. Diele, G. Pelzl, H. Nadasi, and W. Weissflog,

- Phys. Rev. E **63**, 021702 (2003).
- [10] S. Rauch, P. Bault, H. Sawade, G. Heppke, G. G. Nair, and A. Jakli, Phys. Rev. E **66**, 021706 (2002).
- [11] G. Pelzl, S. Diele, and W. Weissflog, Adv. Mater. (Weinheim, Ger.) **11**, 707 (1999).
- [12] Boulder Workshop, Boulder Banana Workshop Archive, <http://anini.colorado.edu/bananas/>
- [13] J. P. Bedel, J. C. Rouillon, J. P. Marcerou, M. Laguerre, M. F. Achard, H. T. Nguyen., Liq. Cryst. **27**, 1411 (2000); **27**, 103 (2000); J. Mater. Chem. **12**, 2214 (2002).
- [14] S. Shubashree, B. K. Sadashiva, and Surajit Dhara, Liq. Cryst. **29**, 389 (2002).
- [15] W. Weissflog, H. Nádasi, U. Dunemann, G. Pelzl, S. Diele, A. Eremin, and H. Kresse, J. Mater. Chem. **11**, 2748 (2001).
- [16] D. S. Shankar Rao, Geetha G. Nair, S. Krishna Prasad, S. Anita Nagamani, and C. V. Yelamaggad, Liq. Cryst. **28**, 1239 (2001).
- [17] J. P. Bedel, J. C. Rouillon, J. P. Marcerou, M. Laguerre, H. T. Nguyen, and M. F. Achard, Liq. Cryst. **28**, 1285 (2001).
- [18] P. Mach, R. Pindak, A.-M. Levelut, P. Barois, H. T. Nguyen, C. C. Huang, and L. Furenid, Phys. Rev. Lett. **81**, 1015 (1998).
- [19] L. S. Matkin, S. J. Watson, H. F. Gleeson, R. Pitney, P. M. Johnson, C. C. Huang, P. Barois, A.-M. Levelut, G. Strajer, J. Pollmann, J. W. Goodby, and M. Hird, Phys. Rev. E **64**, 021705 (2001).
- [20] A. Cady, R. Pindak, W. Caliebe, P. Barois, W. Weissflog, H. T. Nguyen, and C. C. Huang, Liq. Cryst. **29**, 1101 (2002).
- [21] F. Hardouin, H. T. Nguyen, M. F. Achard, and A.-M. Levelut, J. Phys. (France) Lett. **43**, L-327 (1982).
- [22] G. Sigaud, F. Hardouin, M. F. Achard, and A. M. Levelut, J. Phys. (France) **42**, 107 (1981).
- [23] P. Barois, C. Coulon, and J. Prost, J. Phys. (France) Lett. **42**, L-107 (1981).
- [24] P. Barois, Phys. Rev. A **33**, 3662 (1986).
- [25] P. G. de Gennes, and J. Prost, *The Physics of Liquid Crystals*, 2nd ed. (Clarendon Press, Oxford, 1993), p. 557.
- [26] For example, in a Sm- CP_A phase, where the polarization is modulated along the layer normal z , one can write the three components as $p_x \cos(q_0 z)$, $p_y \sin(q_0 z)$ and $p_z \sin(2q_0 z)$. If one sketches the corresponding vector \vec{P} , a helix with a z axis and a two-layers period is found showing the intrinsic helicity of the polarization distribution.
- [27] D. R. Link, J. E. MacLennan, and N. A. Clark, Phys. Rev. Lett. **77**, 11 (1996).
- [28] L. Landau and E. Lifshitz, *Electrodynamics of Continuous Media*, 2nd ed. (Pergamon Press, Oxford, 1984).
- [29] M. F. Achard, J. P. Bedel, J. P. Marcerou, H. T. Nguyen, and J. C. Rouillon, Eur. Phys. J. E **10**, 129 (2003).
- [30] D. M. Walba, E. Körblova, R. Shao, J. E. MacLennan, D. R. Link, M. A. Glaser, and N. A. Clark, Science **288**, 2181 (2000).
- [31] A. Eremin, S. Diele, G. Pelzl, H. Nádasi, W. Weissflog, J. Salfetnikova, and H. Kresse, Phys. Rev. E **64**, 051707 (2002).
- [32] J. Szydłowska, J. Mieczkowski, J. Matraszek, D. W. Bruce, E. Gorecka, D. Pocięcha, and D. Guillon, Phys. Rev. E **67**, 031702 (2003).